TRENDS IN SCIENCES 2025; 22(6): 9591 RESEARCH ARTICLE
https://doi.org/10.48048/tis.2025.9591

Oven-Drying Kinetics and Physical Characterization of Ganyong Starch Biofoam with Various Sizes of Bagasse Filler

Anna Sukma Muthia, Devi Yuni Susanti*, Sri Rahayoe and Khoiri Queen Anyjani

Department of Agricultural Engineering and Biosystems, Faculty of Agricultural Technology, Gadjah Mada University, Yogyakarta 55281, Indonesia

(*Corresponding author's e-mail: deviyunisusanti@ugm.ac.id)

Received: 23 December 2024, Revised: 26 January 2025, Accepted: 2 February 2025, Published: 5 May 2025

Abstract

Biodegradable foam (biofoam) utilizing waste from natural materials and starch as the base and sugarcane bagasse as the filler represents an innovative alternative for controlling the use of polystyrene (PS), commonly known as styrofoam, which has been identified as the 5th most hazardous waste globally by the Environmental Protection Agency (EPA). Using waste from natural materials and starch as the base necessitates further research to produce biofoam with desirable characteristics that are safe for use in food products. Given the intended function of biofoam as a replacement for styrofoam, various factors influencing its characteristics must be considered. This study aims to examine the drying kinetics of biofoam and the effect of sugarcane bagasse particle size on biofoam characteristics. Three particle size variations were used in this study: mesh 60, 80, and 100. The observed physical characteristics parameters include moisture content, density, compressive strength, biodegradability, water absorption, and solubility. The kinetic analysis performs well in representing the data on biofoam moisture content during drying process, evidenced by an R^2 value close to 1 and a low RMSE. All physical characteristics parameters of biofoam, except for moisture content, exhibited improvements proportional to the decreasing particle size of the added sugarcane bagasse. The highest values for each parameter were obtained with the mesh 100 variation, with a density of 0.513 g/cm^3; compressive strength of 12.81 N/mm^2; biodegradability of 60.38 %; water absorption of 54.63 %; and solubility of 58.87 %, while the moisture content for the mesh 100 variation showed the lowest value at 7.86 %.

Keywords: Biofoam, Canna starch, Sugarcane bagasse, Kinetic model, Drying

Introduction

The development of biofoam based on natural materials has recently become a topic that needs to be developed. The development of biofoam is needed as a replacement for the use of styrofoam which has been avoided and reduced in use. Styrofoam or polystyrene foam is a product derived from processed petroleum products. Styrofoam has been widely used in various sectors including the agricultural and food sectors. The use of styrofoam is quite high, especially in food packaging because of some of its advantages such as not easily absorbing water, more economical, and having a sturdy structure, but the high use poses quite serious problems. The content of styrene, which is an active substance derived from benzene, in styrofoam can react if it comes into direct contact with high-temperature food. These toxic substances when mixed with food can attack and cause damage to the nerves of the brain [1-4]. Another negative effect of using styrofoam as food packaging is its nature that is difficult to degrade naturally so that it can harm the environment. As the 5th most hazardous waste in the world by the EPA, several efforts have been made as a measure to control waste or styrofoam waste, namely by recycling, decomposing using plastic decomposing microbes, burial, and burning [5]. However, this handling can cause new problems such as soil and air pollution and the risk of spreading microbes to the environment. One of the alternatives that can be used as a solution in waste control is to create new products that are more environmentally friendly

and have characteristics that are close to *styrofoam* or commonly known as biodegradable foam (biofoam) [6].

The development of biofoam as an alternative to styrofoam is directed at the use of natural materials so that it is expected to degrade back naturally. Generally, the manufacture of biofoam uses starch as the main ingredient because it is easily degraded. The type of starch used comes from ganyong starch which is classified as tubers. Ganyong starch contains fiber and starch with amylose and amylopectin content of 41 and 53 %. This good content encourages ganyong tubers to be an alternative material that can be used in making biofoam [7].

In this study, the manufacture of biofoam will be carried out using ganyong starch combined with sugarcane bagasse as a filler. Bagasse can be used as a filler in the manufacture of biofoam. This is because bagasse contains high cellulose at 46.3 %. High levels of cellulose when converted into a product can have rigid and tough properties and characteristics [8]. In addition to ganyong starch as an adhesive and bagasse as a filler, in the manufacture of this biofoam, Arabic gum (AG) and xanthan gum (XG) are used as stabilizers and thickeners.

As a filler, the size of bagasse particles is suspected to have an effect on the character of the formed biofoam. The characteristics of the resulting biofoam are expected to be close to the characteristics of styrofoam, including weight, flexibility and the level of resistance to water. In addition to the influence of particle size on the character of biofoam, the drying process after printing is also what determines the quality of biofoam. The molding and drying processes can be done separately [5], but they can also be combined such as thermopressing which is commonly used in the manufacture of biofoam [9].

This paper compares several particle sizes to choose the best one to recommend in the application process. The selection of mesh size is not based on other research ranges because there has been no biofoam production research involving mesh size. So, we use sizes 60, 80, and 100 mesh to represent several material conditions, namely fine, medium, and coarse. This research focuses on the formulation and its relation to the characteristics of biofoam. The study aims to examine the kinetics of the biofoam drying process by drying method and the effect of bagasse pellet size on the character of biofoam. This research is expected to provide insight into the drying rate of biofoam based on ganyong starch and bagasse, and serve as a reference for developing formulations and processes to produce high-quality biofoam

Materials and methods

The materials for making biofoam in this study include: Ganyong starch, bagasse, AG, XG, whey protein, and aquaades. The ganyong starch used is produced by MSMEs "Kusuka Ubiku" Banguntapan, Bantul, Yogyakarta, while the bagasse used is the pulp of the green sugarcane type, AG produced by Ingredion, XG produced by Deosen, and whey protein isolate 90. The tools used in making biofoam are SHIMIZU cabinet dryer model PSN-150, VIPOO grinder type V-8300, Tyler mesh sieve 60, 80 and 100 with Endecott-USA vibrator, and Sanyo dryer oven type MOV-112. The tools used in parameter testing include the Brookfield CT3-1000 texture analyzer, the Pioneer Analytical PX224/E type OHAUS analytical balance and the digital micrometer.

The manufacture of biofoam begins with the preparation of materials, especially bagasse fiber. The process of extracting fiber from bagasse begins with washing the bagasse and soaking for 24 h to remove impurities [10]. Then the bagasse is drained and dried using a cabinet dryer with a temperature of 60 °C for 12 h. After drying, the bagasse is combed using a wire comb to separate the cork from the fibers contained in the skin so that it can be taken manually. The bagasse fibers are then ground using a grinder and sieved with a Tyler sieve for 20 minutes. The sieving was carried out with 3 size variations, namely mesh 60, 80 and 100 then the results were taken as a material for making biofoam.

The stages of making biofoam dough begin by mixing the ingredients as presented in **Table 1**, namely ganyong starch, whey protein, AG and bagasse with distilled water. Once the dough is mixed, XG is added and stirred again until the dough is homogeneous.

Table 1 Biofoam composition.

Ganyong Starch (%)	Whey protein (%)	Arabic gum (%)	Xanthan gum 5 % (%)	Distilled water (%)	Bagasse fiber (%)
26.67	11.11	2.44	6.67	42.00	11.11

The biofoam dough is weighed in weight of 15 g and then molded using a melamine cup. After printing, the biofoam sample is dried by baking method at 100 °C for 4 h to reach the condition and obtain an absolute dry value that will be used in the calculation of moisture content (dry basis) [11].

Changes in moisture content during the drying process

In the process of drying biofoam by the baking method, changes in the moisture content of the sample were observed using the thermogravimetric method to identify the drying rate. Observations were made by weighing samples every 20 min for 4 h. After weighing in the last 20 min, the sample was dried at a temperature of 105 °C for 24 h to achieve a balanced moisture content then the data obtained was analyzed with Eq. (1) for wet base moisture content (wb), while for dry base moisture content (db) using Eq. (2). The moisture content data is then re-analyzed to calculate the drying rate of the biofoam.

$$MC\ wb\ = \frac{m_0 - m_1}{m_0} \times 100\ \% \quad (1)$$

$$MC\ db\ = \frac{m_0 - m_1}{m_1} \times 100\ \% \quad (2)$$

Information:

MC wb = Wet base moisture content (%)

MC db = Dry base moisture content (wet base) (%)

m_0 = Initial sample mass (before drying) (g)

m_1 = Final sample mass (after drying) (g)

Biofoam drying rate analysis

The change of moisture content during the constant period of drying is evaluated with Eq. (3). The value of the drying rate is obtained from Eq. (5) The prediction of moisture content in this stage can be determined by Eq. (5).

$$\frac{dM}{dt} = -k \quad (3)$$

$$M_t - M_0 = -k \cdot \mathrm{t} \quad (4)$$

$$M_t = -k.t + M_0 \quad (5)$$

In the profile of the decreasing drying-rate period, the rate of change in moisture content is proportional to the difference between each data of moisture content and the equilibrium moisture content as presented in Eq. (6). The value of the drying rate in this period is determined by Eq. (8) [12]. In this period, the prediction of moisture content can be determined by Eq (9).

$$\frac{\mathrm{dM}}{\mathrm{dt}} = -k(\mathrm{M}_t - \mathrm{M}_e) \quad (6)$$

$$MR = \frac{M_t - M_e}{M_0 - M_e} = e^{-kt} \quad (7)$$

$$Ln\frac{M_t - M_e}{M_0 - M_e} = -k \cdot t \quad (8)$$

$$M_t = M_0 + (M_0 - M_e) \cdot e^{-kt} \quad (9)$$

Model validation tests

Model validation is carried out to determine the suitability between the obtained data and the predicted data. The validity test was determined from the value of the determination coefficient (R^2) and the Root Mean Square Error (RMSE). The R^2 value represents the correlation of the observation value to the prediction in the range of 0 to 1. If the R^2 value is closer to 1, the validity level between the observation data and the prediction will be higher. The RMSE calculation in Eq. (10), is a method to measure the accuracy level of the prediction value as a form of evaluation of the linear regression model so that the smaller the RMSE value It is assumed that the error rate is lower and shows a higher level of accuracy [13,14].

$$RMSE = \left[\frac{1}{N} \cdot \sum_{i=1}^{n} (MR_{exp,1} - MR_{pred,i})^2\right]^{1/2} \quad (10)$$

Characterization of biofoam

Density test

The density testing in this study refers to the ASTM D 792-08 method conducted by [15] namely cutting a biofoam sample with a size of 3×3 cm then multiplying it by the thickness of the sample to obtain a volume value (V), then weighing it using an analytical scale to obtain the sample mass (m). The density (ρ) is calculated by Eq. (11).

$$\rho = \frac{m}{V} \quad (11)$$

Compressive strength test

The compressive strength test in this study refers to the [16] and [17] which is done with the Brookfield texture analyzer (TA) tool connected to the TA-XT Plus software. The type of fixture used is TA-BT-KIT with a TA39 probe, operating at a puncture speed of 0.5 m/s. The data from the compressive strength test, initially recorded as hardness load in kilograms is then converted to tensile stress in N/mm^2 using Eq. (12).

$$\sigma = \frac{load \times \alpha}{\pi \times r^2} \quad (12)$$

Information:

σ = tension (N/mm^2)
load = *hardness load* (kg)
α = acceleration due to gravity (9.81 m/s^2)
π = phi constant (3.14)
r = probe radius (mm)

Biodegradability test

The biofoam degradability test is carried out by burying the biofoam in the soil for 14 days, then weighing before (m_0) and after (m_1) the biofoam is buried in the soil [18].

$$Weight\ Loss\ (\%) = \frac{m_0 - m_1}{m_0} \times 100\ \% \quad (13)$$

Water absorption test

The water absorption test of this study refers to the method used in [15] following the ABNT NBR NM ISO 535 (1999) standard. The sample was cut to a size of 2×2 cm and then weighed to obtain the initial mass (m_0), then immersed in 50 mL of distilled water for 1 minute. After that, the sample is weighed as the final mass (m_t). The percentage of water absorption can be calculated using the Equation. Water absorption is calculated by Equation (9) as follows.

$$\text{Water absorption}\ \ (\%) = \frac{m_t - m_0}{m_0} \times 100\ \% \quad (14)$$

Solubility test

Solubility testing was conducted using the method described by [19] The sample was cut to a size of 2 × 2 cm and weighed to obtain the initial mass (m_0), then dissolved in 50 mL of distilled water. After dissolution, the sample was filtered and dried in an oven for 24 hours. The dried sample was then weighed again to determine the final mass (m_t). The solubility value was calculated using Equation (15).

$$Solubility\ test\ \ (\%) = \frac{m_0 - m_t}{m_0} \times 100\ \% \quad (15)$$

Results and discussion

The Changes of biofoam's moisture content during the oven-drying process

The oven-drying process was carried out to strengthen the interactions between the components of the biofoam. During this process, water evaporates from within the biofoam dough structure into the surrounding air, leading to a reduction in moisture content. The changes in moisture content during the oven-drying process are presented in Figure 1. It can be observed that moisture content decreases with increasing drying time. The moisture reduction in the sample occurs in two distinct phases: a constant drying rate period and a falling rate period. A significant decrease in moisture content is observed at the beginning of the drying process, known as the constant rate period. During this period, the rate of moisture loss is primarily driven by the evaporation of free water from the surface of the biofoam [20].

As the oven-drying process progresses, the free water on the surface of the biofoam becomes depleted due to continuous evaporation, resulting in a slower rate of moisture loss. This phase is referred to as the falling rate period. During this period, the evaporated water originates from the bound water within the biofoam, which migrates to the surface due to differences in vapor pressure. At the same time, the surface moisture content begins to decrease or reaches a critical level known as the equilibrium point. [11].

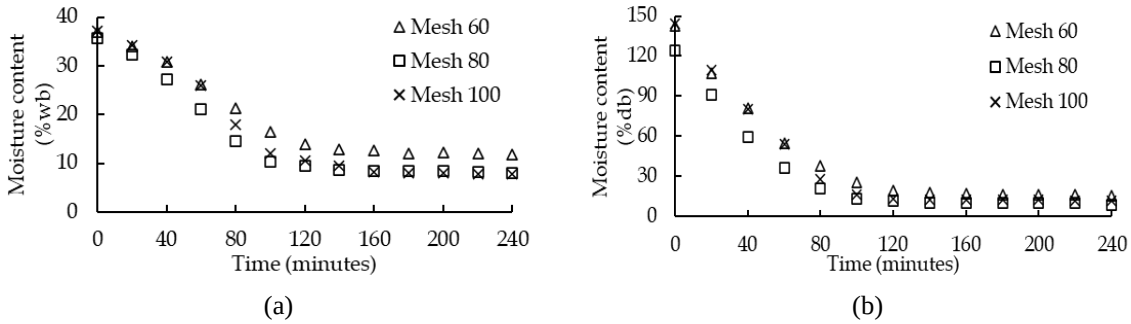

(a) (b)

Figure 1 Rate of change in moisture content during the drying process, (a) *wet* base, (b) *dry* base.

Based on the moisture content data shown in **Figure 1(a)**, it can be observed that during the 240-minute drying process, the drying rate of the biofoam samples from each treatment exhibited both a constant rate period and a falling rate period. Biofoams made with bagasse particle sizes of 60, 80, and 100 mesh had initial moisture contents of 36.98%, 35.65%, and 37.09%, respectively, which decreased to final moisture contents of 11.78%, 8.05%, and 7.86%. The variation in moisture content indicates that particle size has an influence on the rate of moisture content decrease. Therefore, further analysis was conducted to determine the drying rate [21].

Analysis on the constant period and the falling period of drying rate of biofoam

Analysis on the rate of moisture content change was conducted as an indicator of the drying process speed, which is assumed to be influenced by the particle size of the bagasse used as a filler material in the biofoam.

Table 2 Constant values of the drying rate in the constant rate period and the falling rate period

Treatment	k constant (%/min)	k decreases (%/min)
Mesh 60	1.3169a ± 0.0749	0.0071a ± 0.0025
Mesh 80	1.3538ab ± 0.0496	0.0078a ± 0.0027
Mesh 100	1.4603b ± 0.0565	0.0079a ± 0.0044

Analysis on the moisture content's reduction rate during the constant and falling rate periods of the biofoam oven-drying process was conducted applying the dry based moisture content data calculated based on Equation (2). During the constant rate period, the rate constant was determined from the slope of the graph based on Equation (4), while in the falling rate period, the rate constant was obtained from the slope of Equation (8).

Based on **Table 2**, the particle size variation of 100 mesh shows the highest rate constant in both the constant and falling rate periods. This indicates that the drying rate of biofoam with the 100 mesh particle size is faster than that of the other variations, suggesting that smaller particle sizes lead to faster drying rates [22-24].

The predicted drying rate of biofoam was calculated using the rate constants presented in **Table 2**. The drying rate during the constant rate period was predicted using Equation (5), while the falling rate period was calculated using Equation (9). A comparison between the observed and predicted drying rates throughout the drying process is illustrated in **Figure 2**.

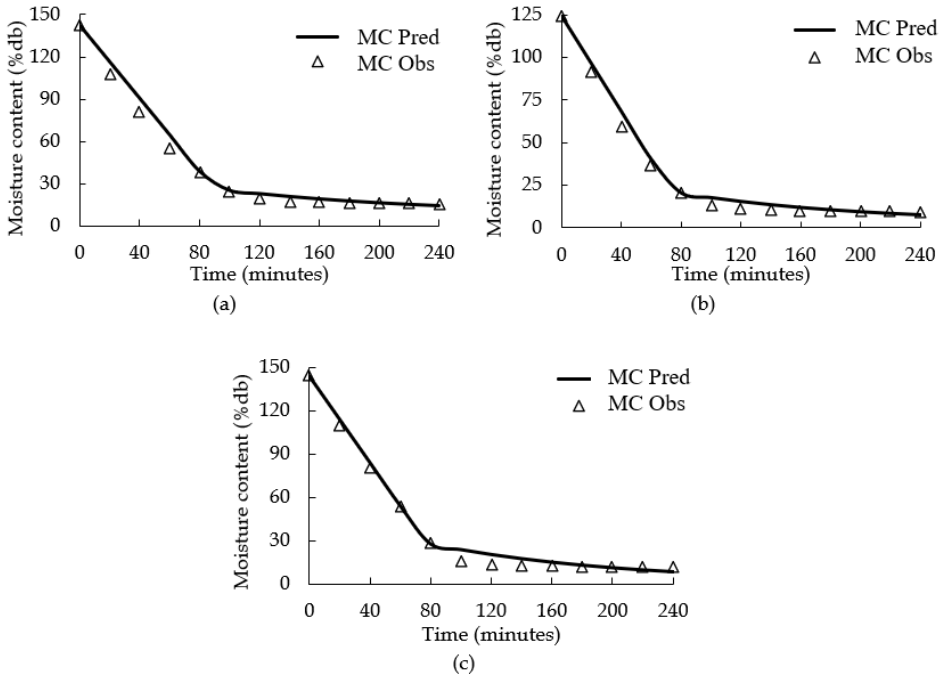

Figure 2 Observed and predicted drying rate of biofoam during the drying process (a) mesh 60, (b) mesh 80, (c) mesh 100.

Based on **Figure 2**, the difference between the observed and predicted moisture content is relatively small. This indicates that the analysis method used to estimate the drying rate for each treatment is appropriate and can effectively represent the observed data. Subsequently, a validation test was conducted to evaluate the model's ability to accurately describe the moisture content changes observed during the drying process.

The Validation of the Drying Kinetics

The validation test of the drying kinetics in simulating the predicted moisture content to the observed moisture content in each variation of bagasse particle size are shown in **Figure 3**. The validation was performed by calculating the R^2 value. The R^2 values which is close to ”1” indicates that the predicted moisture content changes closely represent the observed changes during the drying process [25].

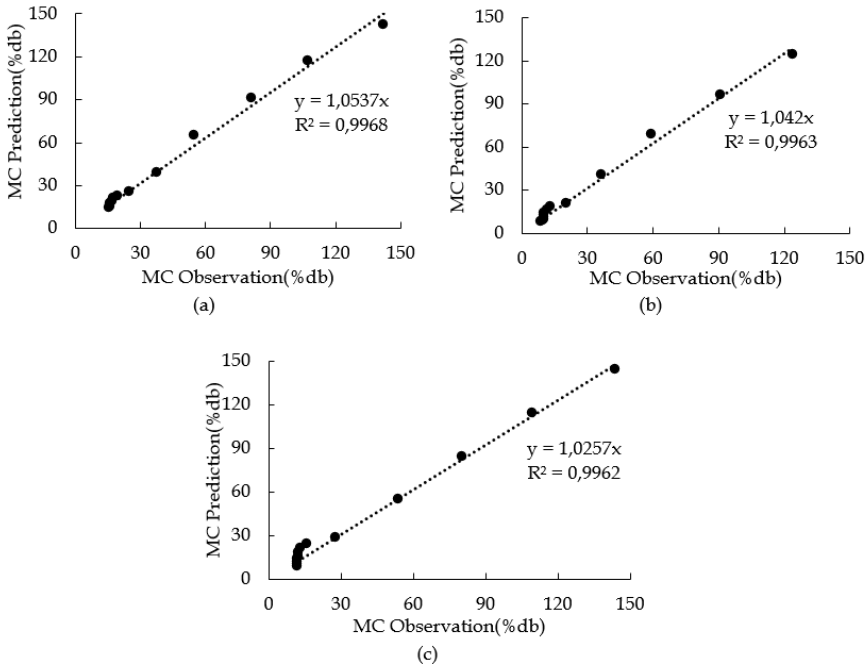

Figure 3 Validation of the prediction model against observed biofoam moisture content using R^2 values for: (a) mesh 60, (b) mesh 80, (c) mesh 100

Table 3 Results of the validation of the drying kinetic

Treatment	R^2	RMSE
Mesh 60	0.9968	4.7493
Mesh 80	0.9963	3.6442
Mesh 100	0.9962	4.0024

The validation results using RMSE can be seen in **Table 3**, where all three treatment variations show relatively low values. This indicates a good agreement between the analysis and the actual data. Based on **Table 3**, the combination of low RMSE values and R^2 values close to 1 suggests that the drying rate analysis performed is accurate and reliable.

Characteristics of biofoam with variations in particle size of sugarcane bagasse

Moisture content of The Biofoam

Moisture content of the biofoam produced using sugarcane bagasse particles of varying sizes as filler is presented in **Figure 4**. Based on the figure, it can be observed that the highest moisture content was found in the biofoam with a particle size of mesh 60, at 11.78%, followed by mesh sizes 80 and 100, at 8.05% and 7.86%, respectively. This indicates a trend where smaller particle sizes result in lower moisture content in the produced biofoam. The smaller particles of sugarcane bagasse provides a larger surface area of drying, which facilitates water diffusion and promotes faster moisture evaporation, resulting in faster drying of the biofoam. [23].

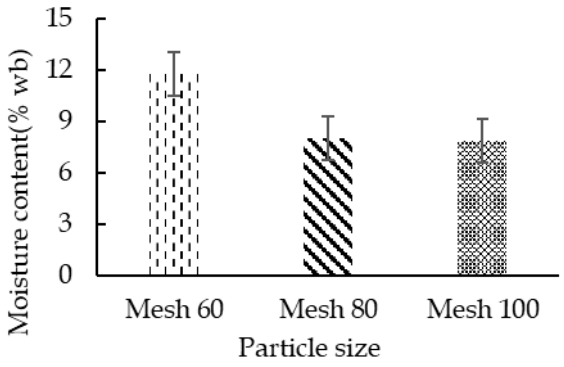

Figure 4 Biofoam moisture content at various particle sizes.

The moisture content in this study ranged from 7.86 to 11.78 %. These results are in line with the findings of Marlina *et al.* [26], who reported biofoam with a moisture content range of 5.99 to 24.9 %. In comparison, the moisture content of polystyrene plastic (Styrofoam) as specified by SNI 06-0177-1987 is only 1.0 %. The difference in moisture content between starch-based biofoam and conventional Styrofoam is attributed to the hygroscopic nature of the biofoam's constituent materials, which readily absorb moisture from the environment. As a result, starch-based biofoam tends to have a higher moisture content.

Density of The Biofoam

Density testing serves as one of the key indicators of the physical quality of biofoam. A lower density value indicates a more porous structure, which in turn affects the physical properties of the resulting biofoam [27]. The density values were calculated using Eq. (11) and are presented in **Figure 5**. The highest density was observed in the biofoam produced with bagasse particles of mesh 100, at 0.513 g/cm³, followed by mesh 80 and mesh 60, with values of 0.509 and 0.488 g/cm³, respectively.

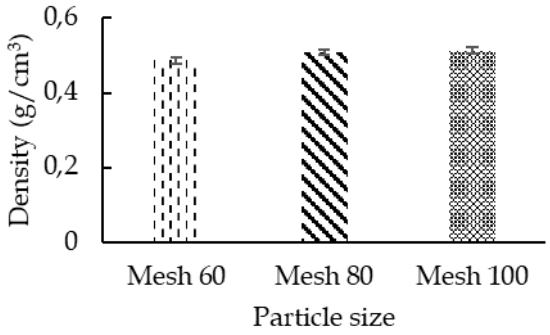

Figure 5 The biofoam density at various particle sizes.

Based on **Figure 5**, it can be observed that the differences in density values among the treatments are not very significant. However, there is a clear trend: the smaller the size of the bagasse particles used, the higher the resulting density. This is because smaller particles reduce the gaps between them, resulting in a denser arrangement of bagasse within the biofoam structure, which in turn increases the overall density [28].

Compressive Strength of The Biofoam

Compressive strength is one of the key parameters used to assess the durability and structural integrity of biofoam, serving as a reference for its effectiveness in protecting products [16]. The addition of fibers in the production of starch-based biofoam aims to enhance its structure and mechanical properties, particularly its compressive strength. Based on the data presented in **Figure 6**, it can be observed that variations in bagasse particle size influence the compressive strength of the

biofoam. There is a clear trend in which smaller particle sizes result in higher compressive strength values [2,28].

The compressive strength was measured using a Texture Analyzer (TA) and calculated using Eq. (12). The highest compressive strength value was recorded for the mesh 100 bagasse particle size variation, at 12.81 N/mm², followed by mesh 80 and mesh 60, with values of 11.20 and 10.31 N/mm², respectively. The compressive strength of biofoam is also influenced by its density. Biofoam with higher density (achieved through the addition of fibers), tends to exhibit greater compressive strength. This occurs because fibers help fill the voids within the matrix material (in this case, ganyong starch), thereby improving both compressive strength and other mechanical properties. [27,29].

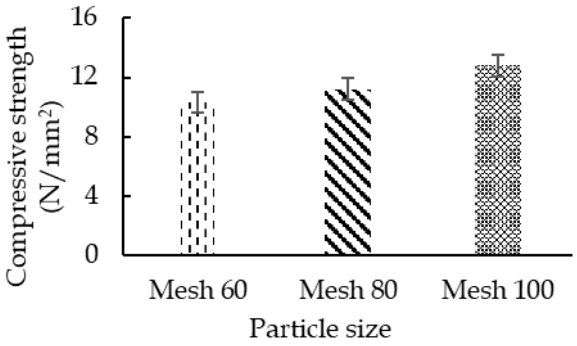

Figure 6 The compressive strength of biofoam at various particle sizes.

Biodegradability of The Biofoam

The biodegradability test aims to determine the amount of material mass lost after burial, which serves as an indicator of whether the produced biofoam can naturally decompose [30]. In addition, this test is conducted to assess the percentage of the sample that is degraded by soil microorganisms [31,32]. Biodegradability was calculated using Eq. (13), and the results are presented in **Figure 7**. The highest biodegradability percentage was observed in the biofoam with bagasse particle size mesh 100, reaching 60.38%, followed by mesh 80 and mesh 60, with biodegradability values of 55.04 and 49.82 %, respectively.

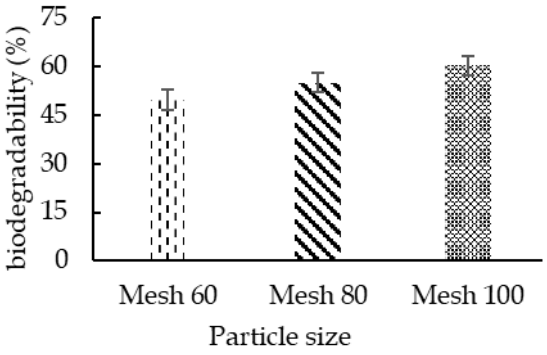

Figure 7 The biodegradability of biofoam at various particle sizes.

Based on **Figure 7**, it can be observed that variations in bagasse particle size influence the biodegradability of the biofoam, with a trend indicating that smaller particle sizes result in higher biodegradability percentages. This occurs because smaller particles increase the surface area, thereby enhancing the availability of substrate and improving the interaction between the biofoam and soil microorganisms, which in turn raises the biodegradability percentage [33]. Biodegradability measurements were conducted on the 14th day of burial, with results showing a biodegradability percentage

ranging from 49.82 to 60.38 %. This indicates that within 14 days, the biofoam sample was able to undergo significant decomposition, although not yet completely degraded. The results of this study comply with the European Union Standard (EN 13432), which stipulates that biodegradable packaging must be capable of decomposing naturally within a maximum period of 6 to 9 months. Moreover, the findings also align with the American Standard Testing and Materials (ASTM D5338), which states that complete degradation of biofoam should occur within 60 days [1,4,16,17].

Water absorption of The Biofoam

Water absorption measurement is one of the key parameters used to assess the quality of biofoam, as it indicates the material's ability and resistance to water exposure. In biofoam applications, this parameter is essential for determining the types of products that can be appropriately packaged using biofoam [34]. The water absorption was calculated using Eq. (14), and the results are presented in **Figure 8**.

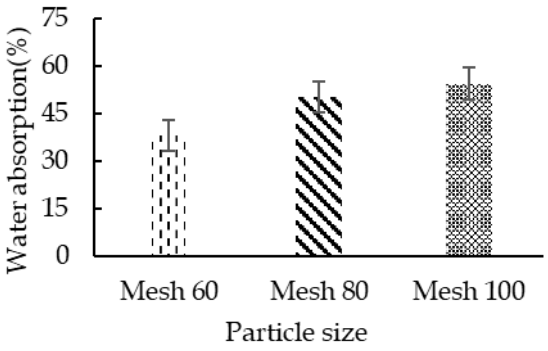

Figure 8 The water absorption of biofoam at various particle sizes.

Based on **Figure 8**, the highest percentage of water absorption was observed in the biofoam with bagasse particle size mesh 100, reaching 54.63 %, followed by mesh 80 and 60, with values of 50.50 and 38.28 %, respectively. The water absorption tends to increase as particle size decreases. This is due to the larger surface area in direct contact with water, which facilitates greater water uptake. Furthermore, during the biofoam manufacturing process, smaller particle sizes may lead to uneven dispersion and agglomeration, resulting in the formation of voids. These voids contribute to the increased water absorption of the resulting biofoam [35,36].

Solubility of The Biofoam

Similar to water absorption, the solubility of biofoam is also a crucial parameter in assessing its quality. Biofoam solubility shows a strong correlation with water absorption capacity. The solubility percentages are presented in **Figure 9**. It can be observed that a higher water absorption percentage tends to correspond with a higher solubility value. The solubility percentage, calculated using Eq (15), reached its highest value in the biofoam with bagasse particle size mesh 100 at 58.87 %, followed by mesh sizes 80 and 60 at 52.71 and 49.89 %, respectively.

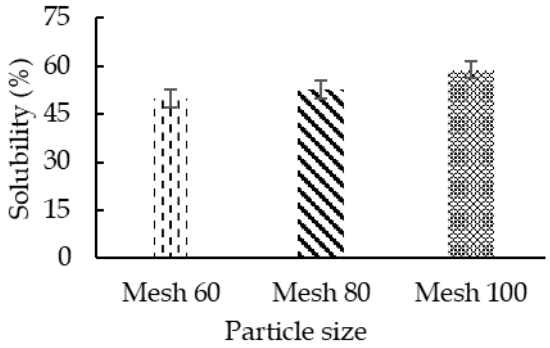

Figure 9 The solubility of biofoam at various particle sizes.

The solubility percentage is also influenced by particle size, which affects the surface area. This is because the dissolution process largely depends on the interaction between the material's surface and the solvent (water, in this case). As a result, biofoam with smaller particle sizes tends to dissolve more easily [37].

Comparative analysis with other biofoam from different raw materials

Comparison of the characteristics of ganyong starch biofoam and bagasse with biofoam made from other materials based on previous research can be seen in **Table 4**. The results of this study indicate that the moisture content remains within the same range as reported by Marlina *et al.* [26]. In terms of density, it can be observed that the density in this study is higher compared to the values reported by Fauzi *et al.* [38] and Sari [6]. The compressive strength of the biofoam produced is higher than that reported by Febriani *et al.* [16] but lower than that of Sumardiono *et al.* [5]. The biodegradability value in this study is relatively high when compared to the findings of Gabriel and Afandi [15]. The water absorption percentage of the biofoam produced in this study tends to be lower than the observations of Ruscahyani *et al.* [39], whereas the solubility value remains within the same range as the biofoam solubility reported by Sari [6]. These variations are attributed to differences in the selection and composition of materials, resulting in distinct characteristics.

Table 4 Comparative Analysis with Other Biofoam from Different Raw Materials

Characteristics of biofoam	Biofoam (ganyong starch + bagasse)	Other biofoam	Material of other biofoam	References
Moisture content (%wb)	7.86 - 11.78	5.99 - 24.9	Paper fiber and orange peel	[26]
Density (g/cm^3)	0.488 - 0.513	0.45 - 1.31	Tapioca and soybean peel flour	[38]
		0.217 - 0.495	Ganyong starch and straw rice	[6]
Compressive Strength (N/mm^2)	10.31 - 12.81	0.0132 - 0.0161	Banana peel starch and bagasse	[16]
		14.162	Tapioca flour and corn fiber	[5]
Biodegradability (%)	45.82 - 60.38 (in 2 weeks)	54.88 - 92.67 (in 4 weeks)	Ganyong starch and straw rice	[15]
Water absorption (%)	38.28 - 54.63	13.93 - 22.38	Tapioca flour and corn husk	[39]
Water solubility (%)	49.89 - 58.87	18.90 - 65.66	Ganyong starch and straw rice	[6]

Production cost at laboratory scale

The biofoam's production cost as shown in **Table 5** is calculated from the production of ganyong starch-based biofoam with the addition of sugarcane bagasse fiber waste at the laboratory scale. The total cost per batch is 0.255 USD, with each batch producing 3 pieces of biofoam with a diameter of 7 cm. This results in a total cost of 0.085 USD per piece. Meanwhile, the price of commercial styrofoam of the same size is 0.093 USD per piece. Therefore, compared to commercial

styrofoam, the biofoam developed in this study shows great potential for industrial-scale production.

Table 5 Calculation of biofoam's production cost.

Components	Unit	Cost (USD)
Ganyong starch (g)	12	0.037
Arabic gum (g)	5	0.050
Xanthan gum (g)	5	0.078
Whey protein (g)	5	0.050
Electricity consumption (kWh)	0.5	0.037
Water consumption (L)	0.5	0.003
Total cost per batch	3	0.255
Total cost per unit	1	0.085

Conclusions

Based on the data analysis and discussion that has been carried out, it was concluded that the change in moisture content of biofoam during the oven-drying process in each treatment showed a constant rate period and falling rate period with a drying constant rate value stretched between 1.3169 to 1.4603 %/min for the constant rate period and between 0.0071 to 0.0079 %/min for the falling rate period with the smaller the size of the bagasse particles added, the larger the constant value indicating the faster the drying rate. The kinetic equation can be used to predict the process of moisture content change during biofoam oven with an R^2 value close to 1 and a fairly low RMSE. The physical characterization of biofoam includes moisture content, density, compressive strength, biodegradability, water absorption and solubility, showing that the smaller the size of the bagasse particles that are added, the higher the physical characterization value of biofoam except for the moisture content which shows that the smaller the particle size, the lower the moisture content of the biofoam produced.

The biofoam produced using ganyong starch and sugarcane bagasse exhibits favorable characteristics, including acceptable moisture content, relatively high density and compressive strength, low water absorption, and good biodegradability. Variations in material composition influence these properties. Additionally, the low production cost compared to commercial styrofoam highlights its potential for industrial-scale application.

Acknowledgements

This research is funded by the Innovative Research Grant Program of the RKAT fund, Faculty of Agricultural Technology at Universitas Gadjah Mada, Indonesian, for the 2023 fiscal year with Work Order number 4074/UN1/FTP.1.3/SET-D/KU/2023 dated July 3, 2023.

References

[1] A Akmala and E Supriyo. Optimasi konsentrasi selulosa pada pembuatan *Biodegradable Foam* dari selulosa dan tepung singkong. *PENTANA* 2020; **1(1)**, 27-40.

[2] AD Cornellia, NA Ashifa, AF Churmelia, SRA Fikri and DO Radianto. Kombinasi jerami dan ampas tebu sebagai biofoam *high durability* dan waterproof dengan metode *mixing* dan *molding*. *KOLONI* 2023; **2(2)**, 49-54.

[3] S Bahri, Fitriani and Jalaluddin. Pembuatan biofoam dari ampas tebu dan tepung maizena. *Jurnal Teknologi Kimia Unimal* 2021; **10(1)**, 24-32.

[4] L Hevira, D Ariza and A Rahmi. Pembuatan biofoam berbahan dasar ampas tebu dan whey. *Jurnal Kimia dan Kemasan* 2021; **43(2)**, 75-81.

[5] S Sumardiono, I Pudjihastuti and R Amalia. Analisis morfologi dan sifat mekanis biofoam dari

tepung tapioka dan serat limbah batang jagung. *Metana* 2021; **17(1)**, 1-5.

[6] GF Sari. The effect of proportion of ganyong starch and waste of straw rice on biodegradable foam production as sustainable packaging. *IOP Conference Series: Earth and Environmental Science* 2022; **1041**, 12003.

[7] DI Lailyningtyas, M Lutfi and AM Ahmad. Uji mekanik bioplastik berbahan pati umbi ganyong (*Canna edulis*) dengan variasi selulosa asetat dan sorbitol. *Jurnal Keteknikan Pertanian Tropis dan Biosistem* 2020; **8(1)**, 91-100.

[8] S Selpiana, P Patricia and CP Anggraeni. Pengaruh penambahan kitosan dan gliserol pada pembuatan bioplastik dari ampas tebu dan ampas tahu. *Jurnal Teknik Kimia* 2016; **22(1)**, 18-24.

[9] P Luna, S Darniadi, A Chatzifragkou and D Charalampopoulos. Biodegradable foams based on extracted fractions from sorghum by-products. *IOP Conference Series: Earth and Environmental Science* 2021; **749**, 12057.

[10] E Indarti, S Muliani, S Wulya, R Rafiqah, I Sulaiman and D Yunita. Development of environmental-friendly biofoam cup made from sugarcane bagasse and coconut fiber. *IOP Conference Series: Earth and Environmental Science* 2021; **711**, 12011.

[11] DY Susanti, WB Sediawan, M Fahrurrozi and M Hidayat. Foam-mat drying in the encapsulation of red sorghum extract: Effects of xanthan gum addition on foam properties and drying kinetics. *Journal of the Saudi Society of Agricultural Sciences* 2021; **20(4)**, 270-279.

[12] DY Susanti, JNW Karyadi and S Mariyam. Drying characteristics of crackers from sorghum using tray dryer in different drying air velocities. *Journal of Advanced Agricultural Technologies* 2016; **3(4)**, 258-264.

[13] A Mahdad, M Benhelal, M Hentabli, S Hanini and M Laidi. Modelling the drying kinetics of apple (Golab variety): Fractional calculus vs semi-empirical models. *Journal of Chemist and Chemical Engineers of Croatia* 2021; **70(5-6)**, 251-262.

[14] D Zhang. A coefficient of determination for generalized linear mixed models. *The American Statistician* 2017; **71(4)**, 310-316.

[15] AA Gabriel and LRP Afandi. Optimization of material formulation and process parameters in canna edulis starch-based biofoam synthesis. *IOP Conference Series: Earth and Environmental Science* 2022; **1114**, 12097.

[16] H Febriani, KIF Kurnia and ZD Pangarso. Pembuatan dan karakterisasi fisik *biodegradable foam* pati kulit pisang dan selulosa ampas tebu. *Jurnal Ilmiah Penalaran dan Penelitian Mahasiswa* 2021; **5(1)**, 1-13.

[17] C Irawan, Aliah and Ardiansyah. Biodegradable foam derived from *Musa acuminate* and *Ipomoea batatas L.* as an environmentally friendly food packaging. *Jurnal Riset Industri Hasil Hutan* 2018; **10(1)**, 33-41.

[18] S Sumardiono, I Pudjihastuti, R Amalia and YA Yudanto. Characteristics of biodegradable foam (bio-foam) made from cassava flour and corn fiber. *IOP Conference Series: Materials Science and Engineering* 2021; **1053(1)**, 12082.

[19] C Togas, S Berhimpon, RI Montolalu, HA Dien and F Mentang. Karakteristik fisik *edible film* komposit karaginan dan lilin lebah menggunakan proses nanoemulsi. *Jurnal Pengolahan Hasil Perikanan* 2017; **20(3)**, 468-477.

[20] PD Ananda, GS Kumar and SA Kumar. Drying kinetics and mathematical modelling of raisin production by abrasive and chemical pre-treatment of grapes. *Journal of Scientific and Industrial Research* 2024; **83(4)**, 350-361.

[21] S Suhendra, F Nopriandy, D Perdana and A Maryam. Analisis kadar air dan laju pengeringan bahan baku pembuatan bubur pedas instan. *Jurnal Engine: Energi, Manufaktur dan Material* 2024; **8(1)**, 22-27.

[22] N Amir, M Efendy, R Hidayat and M Gozan. Analysis and comparison of different dewatering methods on salt quality. *E3S Web of Conferences* 2021; **328**, 5007.

[23] A Daud, Suriati and Nuzulyanti. Kajian penerapan faktor yang mempengaruhi akurasi penentuan. *Lutjanus* 2019; **24(2)**, 11-16.

[24] C Kapseu, DN Bup, C Tchiegang, CF Abi, F Broto and M Parmentier. Effect of particle size and drying temperature on drying rate and oil extracted yields of *Buccholzia coriacea* (MVAN) and *Butyrospermum parkii* ENGL. *International*

Journal of Food Science and Technology 2007; **42(5)**, 573-578.

[25] M Popescu, P Iancu, V Plesu, CS Bildea and FA Manolache. Mathematical modeling of thin-layer drying kinetics of tomato peels: Influence of drying temperature on the energy requirements and extracts quality. *Foods* 2023; **12(20)**, 3883.

[26] R Marlina, Y Sumantri, SS Kusumah, A Syarbini, AA Cahyaningtyas and Ismadi. Karakterisasi komposit *biodegradable foam* dari kemasan pangan. *Jurnal Kimia dan Kemasan* 2021; **43(1)**, 1-11.

[27] P Ferdiansyah, BA Harsojuwono and IW Arnata. Pengaruh konsentrasi asam stearat dan selulosa dari limbah padat pengolahan tapioka terhadap karakteristik biokomposit foam tapioka dan glukomanan. *Jurnal Ilmiah Teknologi Pertanian Agrotechno* 2022; **7(2)**, 114-122.

[28] S Suryaningsih, PM Anggraeni and O Nurhilal. Pengaruh ukuran partikel terhadap kualitas termal dan mekanik briket campuran arang sekam padi dan kulit kopi. *Jurnal Material dan Energi Indonesia* 2019; **9(2)**, 79-85.

[29] A Nugroho, AC Legowo, DM Maharani, Khairunnisa and A Gafur. Physical and mechanical properties of starch foam reinforced with pineapple (*Ananas comosus*) leaves powder. *IOP Conference Series: Earth and Environmental Science* 2022; **1187(1)**, 12016.

[30] J Agus, S Ramadhani, PN Sabrini, DR Wulandari and ZA Ruslan. Development of starch-based biodegradable foam from corn extract with added fiber from banana stems. *Jurnal Chemica* 2023; **42(1)**, 78-86.

[31] E Indarti, S Muliani and D Yunita. Characteristics of biofoam cups made from sugarcane bagasse with *Rhizopus oligosporus* as binding agent. *Advances in Polymer Technology* 2023; **2023**, 8257317.

[32] Rismawati, P Taba and Fahruddin. Study and characterization of biofoam from bagasse (*Saccharum officinarum* L.) with chitosan addition. *Ecological Engineering and Environmental Technology* 2024; **25(7)**, 11-21.

[33] AP Wulandari, E Wulandini and I Indrawati. Biodegradasi jerami padi oleh *Pennicillium* spp. dengan variasi ukuran partikel Jerami. *Jurnal Selulosa* 2014; **4(2)**, 107-113.

[34] FI Muharram. Penambahan kitosan pada biofoam berbahan dasar pati. *Edufortech* 2020; **5(2)**, 118-127.

[35] SC Nwanonenyi and CO Chike-Onyegbula. Water absorption, flammability and mechanical properties of linear low density polyethylene/egg shell composite. *Academic Research International* 2013; **4(1)**, 352-358.

[36] LC Platt-Lucero, B Ramirez-Wong, PI Torres-Chávez, J López-Cervantes, DI Sánchez-Machado, C Reyes-Moreno, J Milán-Carrillo and I Morales-Rosas. Improving textural characteristics of tortillas by adding gums during extrusion to obtain nixtamalized corn flour. *Journal of Texture Studies* 2010; **41(5)**, 736-755.

[37] N Nasirpour and SM Mousavi. Effect of particle size in polyethyltene glycol-Assisted [BMIM][Cl] pretreatment of sugarcane bagasse. *BioEnergy Research* 2021; **14(4)**, 1136-1146.

[38] AR Fauzi, U Sarofa and DF Rosida. Characteristics of biodegradable foam with proportional treatment of tapioca flour and soybean peel flour with added glycerol. *Asian Journal of Applied Research for Community Development and Empowerment* 2024; **8(2)**, 246-253.

[39] Y Ruscahyani, S Oktorina and A Hakim. Pemanfaatan kulit jagung sebagai bahan pembuatan *biodegradable foam*. *Jurnal Teknologi Technoscientia* 2021; **14(1)**, 25-30.